Rheol Acta (2015) 54:817–829
DOI 10.1007/s00397-015-0873-8

ORIGINAL CONTRIBUTION

Structural breakdown and recovery of waxy crude oil emulsion gels

Guangyu Sun[1] · **Jinjun Zhang**[1]

Received: 10 January 2015 / Revised: 18 August 2015 / Accepted: 24 August 2015 / Published online: 5 September 2015

Abstract The structural breakdown and recovery behaviors of waxy crude emulsion gels were investigated. First, the tests of stepwise increase in shear rate and hysteresis loop were carried out, and the structural breakdown process was further analyzed. Then, the structural recovery behaviors were investigated from the recoveries of apparent viscosity, storage modulus, and yield characteristics. It was found that the thixotropy of emulsion gels weakens with increasing water cut and the structural breakdown process gradually changes from solid-like brittle fracture to ductile failure. The broken-down structure of emulsion gels can only recover partially, and both the recovery rate and the recoverability are related to water cut, precipitated wax content, and pre-shear rate. To be specific, the storage modulus recovers faster with increasing water cut and decreasing precipitated wax crystals, or after pre-sheared at a higher rate, while the effects of water cut and precipitated wax on the recovery rate of yield stress are opposite. The recovery degree of both storage modulus and yield stress decreases obviously with increasing amount of wax crystals but is barely influenced by the water cut.

Keywords Waxy crude · Emulsion · Gel · Structure · Breakdown · Recovery

✉ Jinjun Zhang
zhangjj@cup.edu.cn

[1] National Engineering Laboratory for Pipeline Safety / Beijing Key Laboratory of Urban Oil and Gas Distribution Technology, China University of Petroleum (Beijing), 18 Fuxue Road, Changping District, Beijing 102249, China

Abbreviations

t	Time (s)
G'	Storage modulus at time t (Pa)
G'_0	Storage modulus at $t = 0$ (Pa)
G'_∞	Storage modulus at $t = \infty$ (Pa)
t_g	Characteristic gelation time (s)
d	Stretching exponent in Eq. (1) (−)
τ_y	Yield stress at any rest time t after structural breakdown (Pa)
τ_e	Shear stress in the equilibrium, fully broken-down state, i.e., remaining shear stress at the end of the shearing in step (2) of the yield stress recovery test (Pa)
$\tau_{y\infty}$	Recovered yield stress at $t = \infty$ (Pa)
k_{nb}	Recovery rate constant of yield stress in the Nguyen-Boger model (1/h)
K_r	Coagulation rate constant in the Leong model (1/h)
S_{th}	Area enclosed by the up curve and the down curve (Pa s^{-1})
S_{up}	Area determined by the up curve and the shear-rate axis (Pa s^{-1})
S_{down}	Area determined by the down curve and the shear-rate axis (Pa s^{-1})
S_R	Relative thixotropic area (%)
τ	Total shear stress (Pa)
γ	Total shear strain (−)
$\dot{\gamma}$	Shear rate (s^{-1})
λ	Scaled structural parameter, varying between the values of 0 for the completely broken-down structure and 1 for the fully developed structure (−)
G_0	Shear modulus of the completely structured material ($\lambda = 1$) (Pa)

γ_e	Elastic strain of the continuous network structure (−)
Δk	Structure-dependent consistency (Pa s^{n_1})
k	Completely unstructured consistency (Pa s^{n_1})
n_1	Kinetic index describing the viscous stress's dependence on shear rate (−)
p_1,p_2	Dimensionless parameters related to the viscoelastic property (−)
n_2	Positive dimensionless constant (−)
a	Kinetic constant for structure buildup (s^{-1})
b	Kinetic constant for shear-induced breakdown (Pa^{-m} s^{m-1})
ϕ	Rate of energy dissipation, defined as $\phi = \tau\dot{\gamma}$ in the simple shear flow (Pa s^{-1})
m	Dimensionless constant (−)
s	A characteristic time in the elasto-viscoplastic thixotropic model (Eq. 5) with the value of 1 s (s)
τ_{y0}	Yield stress when the gel structure breaks down for the first time (Pa)
τ_{y1h},τ_{y4h},τ_{y8h}	Yield stresses when gel structure yields for the second time after rest for 1, 4, and 8 h, respectively (Pa)

Introduction

In petroleum production systems, water-in-crude oil emulsion is frequently formed due to high shear and flow turbulence encountered at different production facilities (de Oliveira et al. 2010). With the presence of natural surfactants such as resins and asphaltenes, the emulsions can exist with high stability (Kané et al. 2003). The existence of paraffinic wax in the crude oil makes the rheological behavior of the emulsion much complicated because it may precipitate out at low temperature such as the subsea environments and form a network structure (de Oliveira et al. 2010; Paso et al. 2009; Visintin et al. 2008), leading to the gelation of the crude oil emulsions and further flow assurance problems.

The structural breakdown of gelled waxy crude oil occurs under shear. A number of viscoplastic (Guo et al. 2013; Paso et al. 2009; Teng and Zhang 2013a) and elasto-viscoplastic (de Souza Mendes 2009, 2011; Dullaert and Mewis 2006; Mujumdar et al. 2002; Saramito 2009; Teng and Zhang 2013b) models have been developed to describe this structural breakdown behavior. However, only a few studies have been conducted specifically on the structural breakdown behavior of crude oil emulsion gels. The research of Paso et al. (2009) showed that the structural kinetics models proposed for crude oils can also be used for its emulsion gels.

As for the structural recovery of gelled waxy crude oil, different conclusions have been drawn. Some researches held that the structure of waxy crude oil barely recovers after the cessation of shear for many hours (Cheng et al. 2000; Wardhaugh and Boger 1991). However, most researchers reported that partial recovery happened after structural breakdown (Jia and Zhang 2012; Kané et al. 2003; Kané et al. 2004; Rønningsen 1992; Visintin et al. 2005; Wardhaugh and Boger 1987; Webber 2001). Actually, despite the difference in the structural recoverability, the methods for investigating the recovery behavior are very much alike, i.e., monitoring the process of structural growth by the small amplitude oscillation test or by the yield stress evolution with the rest time.

The transition of a material from liquid-like state to solid-like state can be reflected by monitoring the evolution of storage modulus with the rest time after shearing (de Kretser and Boger 2001). The advantage of this method is that it does no harm to the structural recovery process. Therefore, it has been widely used in studying the structural recovery of structured fluids, such as sodium montmorillonite suspensions (Sohm and Tadros 1989), mineral suspensions (de Kretser and Boger 2001), clay particle-stabilized emulsions (Whitby and Garcia 2014), laponite-stabilized emulsions (Garcia and Whitby 2012), drilling muds (Yap et al. 2011), etc. Based on the time evolution of storage modulus, a structural buildup model was developed by Visintin et al. (2005) to quantitatively characterize the rate of structural recovery, as shown in Eq. (1).

$$\frac{G'-G'_0}{G'_\infty-G'_0} = 1-\exp\left[-(t/t_g)^d\right] \tag{1}$$

In this equation, t_g means the reciprocal of the rate constant for gelation; d reflects the sensitivity of G' on t. To analyze the influence of the stretching exponent d, the storage modulus and the time are non-dimensionalized to eliminate the effects of different values of G'_∞ and t_g. The evolutions of G'/G'_∞ with t/t_g at different values of d are demonstrated in Fig. 1. As can be seen, in the range of 0 and 1, the smaller the d is, the

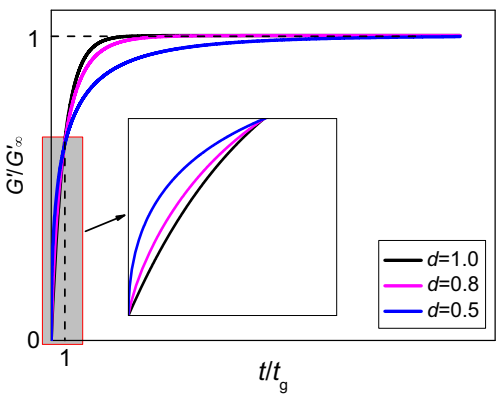

Fig. 1 Schematic of the influence of d on the growth of G' in Eq. (1)

faster the storage modulus increases at the beginning and the slower at the later period.

Moreover, structural recovery can also be presented by the increase of yield stress after different rest times. The advantage of this method is that yield stress is a significant parameter in industrial applications and relevant to real process, making this method easy to interpret (de Kretser and Boger 2001). Though this method has been employed in many fields (de Kretser and Boger 2001; Levy 1962; Nguyen and Boger 1985; Solomon et al. 2001; Van Kessel and Blom 1998), it has not been used in the study of the structural recovery behavior of crude oil emulsion gels yet.

In literatures, two yield stress recovery models were proposed to describe the aging of different materials. One of them was developed by Nguyen and Boger (1985) for the modeling of the recovery of bauxite residue suspensions, which can be expressed as

$$\tau_y(t) = \tau_{y\infty} - \left(\tau_{y\infty} - \tau_e\right) e^{-k_{nb}t} \tag{2}$$

The other was put forward by Leong (1989) for the recovery of brown coal suspensions on the assumption that the evolution of yield stress is attributed to the change of the particle bond concentration. The model is represented as

$$\tau_y(t) = \tau_{y\infty}\left(1 - \frac{1 - \left(\frac{\tau_e}{\tau_{y\infty}}\right)^{3/2}}{1 + K_r t}\right)^{2/3} \tag{3}$$

The Nguyen-Boger model and the Leong model are based on the first-order and the second-order chemical reaction kinetics for structural reformation, respectively.

This paper concerns the structural breakdown and recovery behaviors of waxy crude oil emulsion gels. First, the experiments of stepwise increase in shear rate were performed, and the structural breakdown process was investigated and compared between waxy crude oil and its emulsion gels with the help of an elasto-viscoplastic thixotropic model. Then, the structural recovery behaviors were studied by analyzing the evolution of viscosity after the stepwise decrease in shear rate, the evolution of storage modulus with the time of rest, and the growth of yield stress after different rest time, respectively.

Experimental section

Materials and emulsion preparation

A typical waxy crude oil produced in China was employed to prepare emulsions. The physical properties of the crude oil are listed in Table 1. For detailed determination methods of these parameters, one may refer to our previous article (Sun et al. 2014). The water used was ultrapure water, and no emulsifier was added.

Table 1 Physical properties of the studied waxy crude oil

Parameter	Value
Density at 20 °C (kg/m^3)	876.6
Pour point (°C)	35.0
Gelation temperature (°C)	32.4
WAT (°C)	44.3
Wax (wt.%)	20.73
Resins (wt.%)	7.07
Asphaltenes (wt.%)	1.41

The procedures for the preparation of the crude oil emulsions were the same as those in our article (Sun et al. 2014).

Rheological measurements

All rheological measurements in this study were performed by a HAAKE Mars III rheometer (Thermo Fisher Scientific Inc., Germany) equipped with the Z38TiP coaxial cylinder geometry. The temperature of the sample in the geometry was controlled by a HAAKE AC200 circulating water bath (Thermo Fisher Scientific Inc., Germany) with the accuracy of 0.01 °C.

The structural breakdown behaviors were studied by two methods: stepwise increase in shear rate and hysteresis loop.

Stepwise increase in shear rate

The test proceeded as follows. The measuring system was first heated at 50 °C, and then the sample was loaded and kept for 10 min before it was cooled to the test temperature at a rate of 0.5 °C/min and maintained at that temperature for 1 h to ensure the structure reached equilibrium. Then stepwise increase in shear rate was applied with the shear rate being 1, 2, 4, 8, 16, and 32 s^{-1} in turn. The duration at each shear rate was 10 min.

Hysteresis loop test

The sample loading, cooling, and isothermal procedures were identical with those of the shear-rate stepwise increase test. The shear rate was changed from 0 to 50 s^{-1}, and then back to 0 s^{-1} at a rate of 1 s^{-1}/s. After the first loop, the shearing program was immediately repeated once to obtain the second hysteresis loop. The actual loading procedure of the shear rate is demonstrated in Fig. 2.

As to the studies on structural recovery behaviors, the small-amplitude oscillatory shear (SAOS) and the yield stress measurement were both employed. The specific testing procedures will be described in "Structural recovery behaviors."

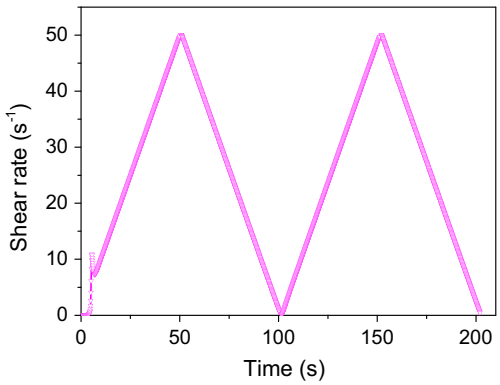

Fig. 2 Input of hysteresis loop test

Results and discussion

Thixotropic behaviors of waxy crude oil emulsion gels

Although controversy remains all along about whether or not the partially recoverable structured fluids could be called thixotropic fluids (de Kretser and Boger 2001; Mewis and Wagner 2009; Nguyen and Boger 1985; Roussel 2006), the term "thixotropy" is still used in many works (Davidson et al. 2007; Kané et al. 2004; Vinay et al. 2005, 2007). We follow this usage here.

The impact of water cut on the thixotropic behaviors of emulsion gels was explored first. The stress evolutions of crude oil and its emulsion gels in the shear-rate stepwise increase test are illustrated in Fig. 3. The hysteresis loops are illustrated in Fig. 4. Both Figs. 3 and 4 show that the deformation of the emulsion gel is qualitatively similar to that of the crude oil, except that the structural strength is obviously increased with increasing water cut. One thing to be explained is the reason why multiple values for the shear stress at the same shear rate were obtained in the beginning of the hysteresis loop tests in Fig. 4c. This is due to the limitation of the rheometer. In this study, the strain-controlled hysteresis loop tests were conducted by HAAKE Mars III—a stress-controlled rheometer. As is known, the strain-controlled mode is still achieved by the control of stress provided by the motor.

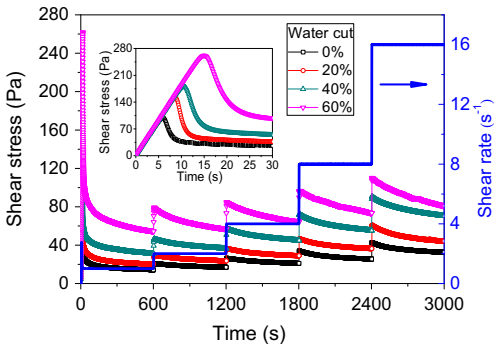

Fig. 3 Shear stress vs. time of crude oil and its emulsion gels in the shear-rate stepwise increase test at 26 °C

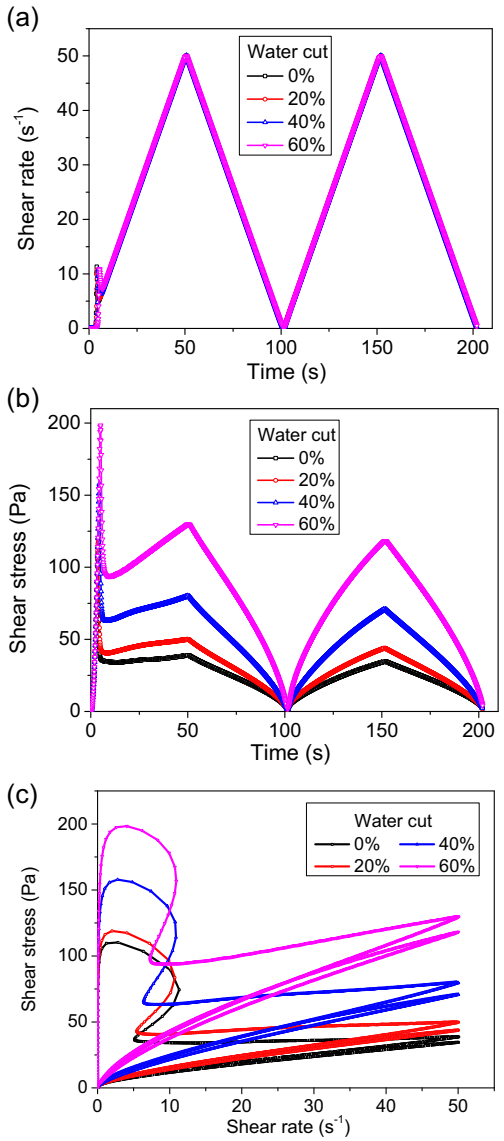

Fig. 4 Hysteresis loops of crude oil and its emulsion gels at 31 °C. **a** Input: measured shear rate with time. **b** Output: measured shear stress with time. **c** Hysteresis loop: measured shear stress vs. measured shear rate

Consequently, when the structure of the sample changes dramatically, the feedback speed of stress is unable to keep pace with the change of structure, so the phenomenon that the shear rate decreases may appear. Figure 4a, b are the parametric representations of the shear rate and the shear stress with time as independent parameter, respectively, which shows clearly that the shear rate at the onset is unstable.

The influence of temperature on the thixotropic behaviors of emulsion gels may be found in Figs. 5 and 6. It can be seen that both the structural strength and the thixotropy of emulsions are obviously increased with decreasing temperature, i.e., increasing amount of precipitated wax. Similar to Fig. 4, the shear rate at the onset of the hysteresis loop test is also unsteady, as can be seen in Fig. 6a.

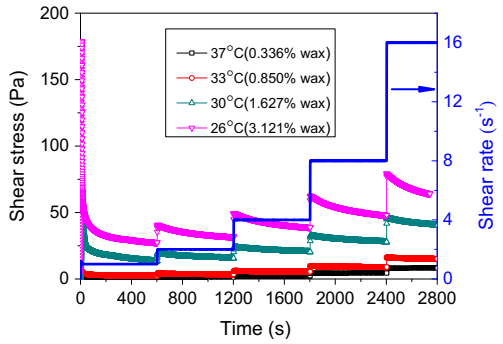

Fig. 5 Shear stress vs. time of the 30 % water cut emulsion in the shear-rate stepwise increase test at different temperatures

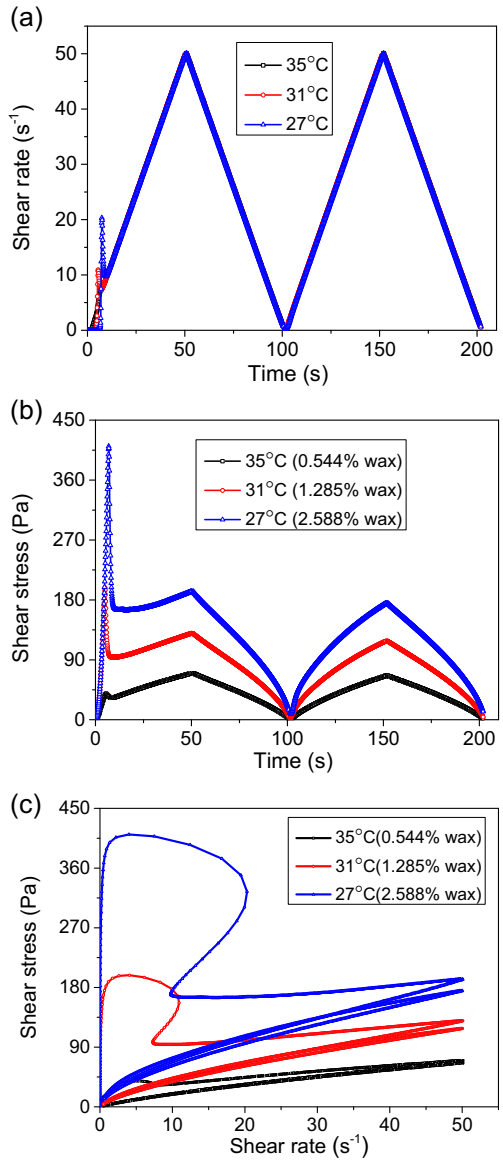

Fig. 6 Hysteresis loops of the 60 % water cut emulsion at different temperatures. **a** Input: measured shear rate with time. **b** Output: measured shear stress with time. **c** Hysteresis loop: measured shear stress vs. measured shear rate

The relative thixotropic area S_R (Dolz et al. 2007; Hernández et al. 2008; Tárrega et al. 2004) was employed to analyze the results of hysteresis loop tests and further to explore the contributions of dispersed water and precipitated wax to the thixotropic behaviors of emulsion gels.

$$S_R(\%) = \frac{S_{th}}{S_{up}} \times 100 = \frac{S_{up} - S_{down}}{S_{up}} \times 100 \tag{4}$$

As shown in Table 2, the thixotropic areas of both the first loop and the second loop monotonically increase with increasing water cut, but the relative thixotropic area of the first loop decreases. These results indicate that the thixotropy of emulsion gel is actually weakened with increasing water cut although the structure is strengthened at the same time. The weakening of the thixotropy of emulsion gel results from the increasing ratio of dispersed water to precipitated wax, because at the same temperature, the total amount of precipitated wax at a higher water cut is less than that at a lower water cut due to the lower proportion of oil phase. The effect of water-to-wax ratio is also verified by the decrease of the relative thixotropic areas with increasing temperature in Table 2. More specifically, the amount of precipitated wax is less at higher temperature when the water cut remains the same.

Meanwhile, it is observed that the relative thixotropic area of the second loop remains in the interval of 6–7 %, which is much less than that of the first loop and almost invariable with water cut. This reflects that the recoverability of the waxy crude oil and its emulsion gels is quite weak and almost independent of water cut. This independence was also found in yield stress, which will be discussed later.

The rheology of waxy crude oil has been intensively studied, and more recently, an elasto-viscoplastic thixotropic model (Teng and Zhang 2013b) was developed by our research group for waxy crude oil. This model can well depict "the complete transient flow curve, from the initial elastically dominated region, through the viscoelasticity and thixotropy coexistence region accompanied by a yielding process, and finally to the viscously dominated region after yielding." The model is as follows:

$$\begin{cases} \tau = \lambda G_0 h(\gamma_e)\gamma_e + (1-\lambda)\cdot(\lambda\Delta k + k)\dot{\gamma}^{n_1} \\ h\ (\gamma_e) = \dfrac{1}{1 + p_1 \cdot \gamma_e^{p_2}} \\ \dfrac{d\lambda}{dt} = \dfrac{1}{1+\gamma^{n_2}}\left[a(1-\lambda) - b\lambda\phi^m\right] \\ \dfrac{d\gamma_e}{dt} = \left[g_1 - (1-g_1)s\dot{\lambda}\right]\dot{\gamma} \\ g_1 = \exp\left[-(p_1\cdot\gamma^{p_2})\right] \end{cases} \tag{5}$$

Given that the rheological response of emulsion gel is similar to that of crude oil, we try to apply this model to emulsion gels. The fitted results of the flow curves in Fig. 3 are demonstrated in Fig. 7, and the model parameters are listed in

Table 2 Thixotropic areas and relative thixotropic areas of crude oil and its emulsion gels

Temperature (°C)	Water cut (vol%)	First hysteresis loop			Second hysteresis loop		
		S_{up} (Pa·s^{-1})	S_{th} (Pa·s^{-1})	S_R (%)	S_{up} (Pa·s^{-1})	S_{th} (Pa·s^{-1})	S_R (%)
31	0	3072.2	1956.2	63.7	1085.8	67.5	6.2
	20	3524.3	2127.4	60.4	1353.3	89.3	6.6
	40	5102.9	2887.6	56.6	2160.6	158.6	7.3
	60	7182.1	3450.6	48.0	3674.1	237.9	6.5
27	60	17,391.1	11,666.8	67.1	5708.3	444.0	7.8
35		2454.7	513.2	20.9	1919.9	57.2	3.0

Table 3. As shown in Fig. 7, both the viscoelastic deformation before yielding and the thixotropic behaviors after yielding can be well described by this model. Likewise, the fitted results of the hysteresis loop curves in Fig. 4c are shown in Fig. 8. As demonstrated above in Fig. 4a, the data are unsteady at the onset of shearing, so only the data after time >25 s are used for model fitting. The fitted model parameters are listed in Table 4.

It can be seen from Tables 3 and 4 that G_0, Δk, and k increase monotonically with increasing water cut, which clearly indicates the structural enhancement by dispersed droplets. Meanwhile, the parameter n_1 decreases with increasing water cut, showing that the dependence of viscous stress on shear rate is reduced, i.e., the emulsions become more non-Newtonian.

The structural parameter λ and the overall structural breakdown rate $d\lambda/dt$ can be calculated by using the model. The evolutions of λ and $d\lambda/dt$ of crude oil and its emulsion gels in Fig. 7 are shown in Figs. 9 and 10, respectively. Based on Figs. 9 and 10, the following conclusions can be reached according to the evolution of the structural parameter and its breakdown rate with increasing water cut.

(1) After only 1 s or so, the structure of the crude oil starts to break down first. The crude oil is also the first material to reach the maximum breakdown rate and approximate equilibrium ($d\lambda/dt$ in close proximity to 0). This indicates that the structure of the crude oil is more brittle than that of its emulsion gels. (2) The dispersed droplets make the emulsion gels gradually become ductile. To be specific, as the water cut increases, the structural breakdown begins later and later, and so is the moment at which the $d\lambda/dt$ reaches its maximum, and the peak value of $d\lambda/dt$ gradually decreases. The enhancement of ductility agrees with our previous observation on the yielding behavior of emulsion gels (Sun et al. 2014).

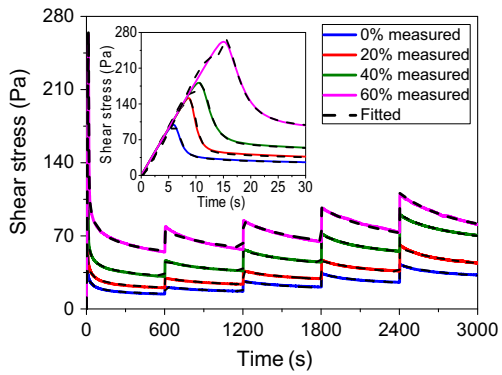

Fig. 7 Model-fitting results of shear-rate stepwise increase tests at 26 °C for crude oil and its emulsion gels

With the assistance of the model, the evolution of the elastic strain can also be obtained, as shown in Fig. 11. Before and around the yielding of the structure, waxy crude oil and its emulsion gels mainly present elasticity, and during this phase the elastic strain accounts for a high proportion of the total strain. Therefore, when the sample structure yields at 10 s or so, the elastic strain increases dramatically due to the rapid increase of the total shear strain. After the yielding of the structure, the increasing rate of the elastic strain slows down because the sample becomes viscous fluid. For all the samples, the elastic strain only increases from about 1.5 to no more than 2.5 when the total shear strain increases from about 18 to about 18,600, demonstrating the weak elasticity remaining in the samples. Furthermore, it can be seen that the elastic strain decreases with increasing water cut, which may result from the breakage of water droplet clusters and further the coalescence of droplets in the sheared emulsion gels. This could lead to the weakening of elasticity and the increase of unrecoverable viscous strain, as proved by the effect of water cut on the strain recovery after yielding in the previous research (Sun et al. 2014).

Structural recovery behaviors

Viscosity

The recovery of apparent viscosity for gelled waxy crude oil was investigated in the following procedures. (1) The sample in the rheometer was cooled to 31 °C from 50 °C at a rate of 0.5 °C/min and kept for 1 h. (2) The sample was sheared at the rate of 1, 10, and 100 s^{-1} for 30 min, respectively. (3) The shear rate was lowered to 0.5 s^{-1} immediately and kept for 1 h, and the recovery process of the apparent viscosity was recorded.

Table 3 Fitted model parameters from shear-rate stepwise increase tests of crude oil and its emulsion gels at 26 °C

Water cut (vol%)	G_0 (Pa)	Δk (Pa s^{n_1})	k (Pa s^{n_1})	n_1 (–)	n_2 (–)	a (s^{-1})	b ($Pa^{-m}\cdot s^{m-1}$)	m (–)	p_1 (–)	p_2 (–)	AADs (%)
0	2251.8	71.65	1.76	0.824	0.843	0.0118	0.0139	0.854	34.86	1.49	1.36
20	3678.7	116.77	2.31	0.790	0.885	0.0043	0.0063	0.969	31.11	1.42	2.29
40	4127.3	154.17	5.31	0.756	0.886	0.0039	0.0054	0.974	29.06	1.38	2.83
60	4323.0	252.42	6.57	0.661	0.870	0	0.0009	1.137	21.01	1.43	3.56

As illustrated in Fig. 12a, the recovery process of the viscosity of water-free crude oil is significantly affected by the pre-shear condition. There is an obvious recovery process after the high pre-shear at the rate of 100 s^{-1}, while the viscosity barely recovers after the pre-shear at the rate of 10 s^{-1} or lower. Clearly, this is related to the different degrees of damage to wax crystal network structure caused by the different pre-shear conditions. Only when the structure is damaged to a certain degree will the viscosity begin to recover obviously.

It can also be observed from Fig. 12a that the final recovered viscosity is influenced by the rate of pre-shear. The higher the pre-shear rate is, the lower is the finally recovered apparent viscosity at 0.5 s^{-1}. This indicates that the structure of waxy crude oil cannot fully recover within the test time after severe breakdown, and the degree of structural recovery is related to the degree of structural damage. This is a rheological behavior different from the traditional definition of thixotropy.

When the same test is performed on the 40 % water cut emulsion gel, it can be seen from Fig. 12b that the overall structural recovery behavior of emulsion gel is similar to that of crude oil. That is, the partial recovery may occur which is related to the degree of structural damage. What is different from the crude oil is that the viscosity of the 40 % water cut emulsion gel shows obvious recovery after pre-sheared at 10 s^{-1}, while the crude oil shows little recover in viscosity after pre-sheared at this shear rate.

As mentioned above, the structural recovery behaviors of emulsion gels are dependent on water cut, pre-shear condition, etc. This will be discussed below from the view of viscoelasticity and yielding behavior.

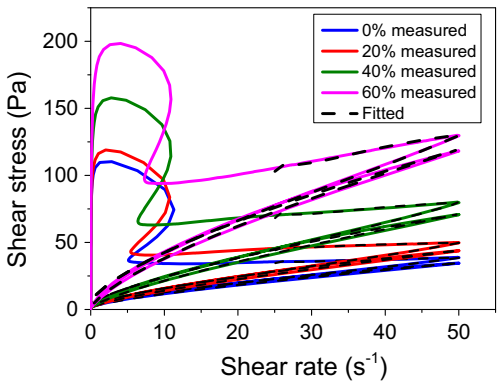

Fig. 8 Model-fitting results of hysteresis loops at 31 °C for crude oil and its emulsion gels

Viscoelasticity

The recovery of emulsion gel structure was investigated by SAOS in the following procedures. (1) The sample in the rheometer was cooled to 31 °C from 50 °C and kept for 1 h to ensure that the structure built up to reach equilibrium. During the isothermal process, the SAOS was applied at a constant frequency of 1 Hz to track the structural buildup, and the strain amplitude was set as 0.0002 to ensure the deformation within the linear viscoelastic limit. (2) Then the constant shear rate of 100 s^{-1} was applied for 30 min to break the structure of the sample. (3) After structural breakdown, the SAOS test was performed again for 2 h to monitor the viscoelastic recovery with rest time.

As can be expected, during the process of structural buildup, i.e., in step (1), the storage moduli of the crude oil and the emulsion gels increase continuously with time. The growth of storage modulus can be modeled by Eq. (1) and the results are shown in Table 5. As can be seen, the characteristic gelation time t_g shortens with the increase of water cut, indicating that the structural buildup quickens. This is in accordance with our previous study (Sun et al. 2014).

During the structural recovery process, i.e., in step (3), the storage moduli of the fractured crude oil and emulsion gels also increase with rest time. This process can be well described by Eq. (1) as well, as shown in Fig. 13a. The fitted parameters are listed in Table 6.

The same test was performed at a lower temperature, i.e., 28 °C, for crude oil and its emulsion gels. The recoveries of storage moduli after structural breakdown are shown in Fig. 13b, and the fitted parameters are also listed in Table 6.

As can be seen, the fitted G_0' of both the crude oil and the emulsion gels, i.e., the storage moduli at the moment when the shearing is stopped, are 0 Pa. Actually, the measured values are also below 0.5 Pa. This phenomenon indicates that the shearing results in the complete breakdown of wax crystal structure. During structural recovery process, the characteristic gelation time t_g shortens with the increase of water cut. That is to say, the viscoelastic recovery quickens as the contribution of dispersed droplets to the gel structure increases. This is opposite to the structural breakdown process, i.e., the structural breakdown becomes slower and recovery becomes quicker with the increase of dispersed water.

Table 4 Fitted model parameters from hysteresis loops of crude oil and its emulsion gels at 31 °C

Water cut (vol%)	G_0 (Pa)	Δk (Pa s^{n_1})	k (Pa s^{n_1})	n_1 (−)	n_2 (−)	a (s^{-1})	b ($Pa^{-m}\cdot s^{m-1}$)	m (−)	p_1 (−)	p_2 (−)	AADs (%)
0	1363.6	2.36	2.01	0.873	0.465	0.0188	0.0020	0.887	42.55	1.05	1.12
20	1826.9	3.20	2.34	0.814	0.438	0.0135	0.0011	0.966	38.82	1.05	1.34
40	2429.6	3.54	3.56	0.760	0.190	0.0010	1.7×10^{-5}	1.223	25.35	1.03	2.07
60	3478.1	5.69	7.34	0.710	0.077	0	7.2×10^{-7}	1.466	16.96	1.02	2.56

By comparing Tables 6 and 5, one can see that G'_∞ is much less than that before shearing. The recovery proportion is almost independent of the water cut and only about 10 %, which is below the proportion (15–25 %) obtained by Visintin et al. (2005) in the study of waxy crude oil, but above that (about 3 %) by Kané et al. (2004). This implies that the recoverability of the structure of crude oil and its emulsion gels is not definite, but variable from oil to oil.

Further, it can be seen that t_g increases with the fall of temperature (i.e., the increased amount of precipitated wax), which means that the duration of structural recovery lasts longer as more paraffin wax precipitates out.

When the shear rate in step (2) was reduced to 10 s^{-1}, the recovery process of storage modulus was changed, with the fitted parameters shown in Table 6 as well. The following can be deduced by comparing the recovery processes after 100 and 10 s^{-1}.

1. The maximum storage moduli that can be reached after recovery are roughly the same. This is consistent with the result of waxy crude oil by Visintin et al. (2005).
2. The storage modulus recovers faster after the gel structure is sheared at a higher rate. As we know, when shear equilibrium is reached at a specific shear rate, the breakdown rate of the gel structure equals the recovery rate. The structure breaks down faster when sheared at a higher shear rate, and correspondingly the structure has to recover faster. Therefore, when the shear is stopped, the structure continues to recover faster due to inertial effect.
3. The higher the water cut is, the less the recovery process of storage modulus varies with the pre-shear rate. This conclusion can be easily obtained by comparing the differences of the parameters t_g and d between the two processes at a lower water cut with the differences at a higher water cut. This is because the contribution of dispersed droplets to the gel structure increases with increasing water cut, but no recovery happens in droplets after shear. The latter is demonstrated in Fig. 14 which shows that the storage modulus of the emulsion above WAT does not grow up with rest time after shear, meaning that it is the wax crystal rather than the droplets that leads to the structural recovery of emulsion gels.

It can also be seen from Table 6 that the stretching exponent d decreases with the increase of water cut, the decrease of temperature, and the reduction of pre-shear rate. That is to say, the structure of waxy crude oil emulsion gels recovers faster in the beginning of the recovery process and slower in later period when there are more water droplets dispersed or more paraffinic wax precipitated in the emulsion gels, or the emulsion gels are pre-sheared by a relatively lower shear rate.

Yield behavior

In order to investigate the structural recovery behaviors of emulsion gels during a long time of rest, the yield behavior was employed as an indicator, and the test procedures were as follows. (1) The samples were cooled to 31 °C (or 28 °C) from

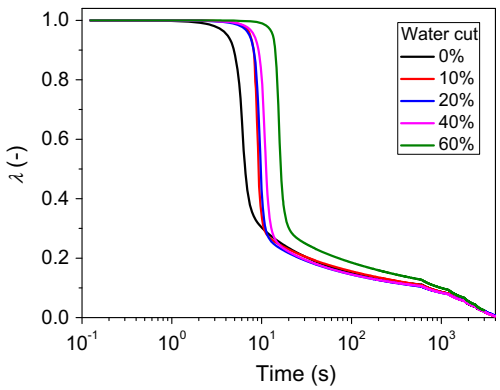

Fig. 9 Evolution of the structural parameter for crude oil and its emulsion gels under shear-rate stepwise increase test at 26 °C

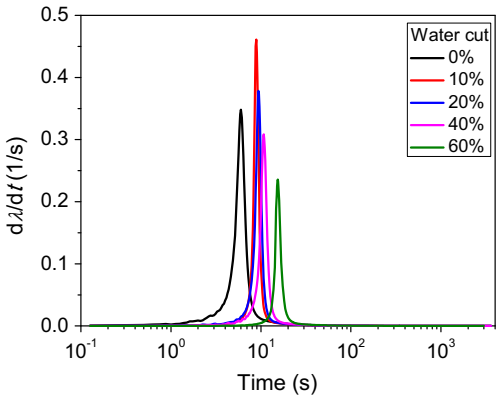

Fig. 10 Evolution of the structural breakdown rate for crude oil and its emulsion gels under shear-rate stepwise increase test at 26 °C

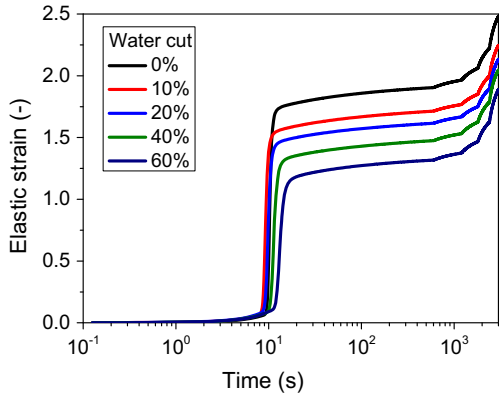

Fig. 11 Evolution of the elastic strain for crude oil and its emulsion gels under shear-rate stepwise increase test at 26 °C

50 °C at a rate of 0.5 °C/min and kept for 1 h. (2) The constant shear rate of 0.1 s^{-1} was applied for 30 min to make sure that the gel structures were broken down. (3) After that, the samples were kept at rest to allow structural recovery for 1, 4, and 8 h, respectively. (4) The constant shear rate of 0.1 s^{-1} was applied again, and accordingly the recovered structures yielded for the second time. The details of the methods for determining yield stress and yield strain were introduced in our previously published article (Sun et al. 2014).

The results are shown in Fig. 15, from which it can be drawn that the maximum value of τ_e/τ_{y0} appears at the water-free crude oil, and the recovery proportion, i.e., τ_{y1h}/τ_{y0},τ_{y4h}/τ_{y0} and τ_{y8h}/τ_{y0}, of the crude oil is higher than those of the emulsion gels during the whole recovery process. This is due to the coalescence of droplets when the emulsion gels were subjected to shearing, and the droplets play no part in recovery as mentioned above (Fig. 14), which results in the poorer recovery of emulsion gels.

After verification, the Nguyen-Boger model, rather than the Leong model presented in the Introduction, can be used to describe the relation between the yield stress and the rest time, indicating that the structural recovery process of waxy crude oil emulsion gels obeys the first-order kinetics. The fitting results are shown in Table 7.

Table 5 Fitted parameters of Eq. (1) for crude oil and its emulsion gels during the isothermal process at 31 °C

Water cut (vol%)	G_0' (Pa)	G_∞' (Pa)	t_g (s)	d	R^2
0	95.8	1066.7	1110.7	0.902	0.9995
10	156.9	1889.7	1009.8	0.850	0.9993
20	189.1	2037.5	909.1	0.774	0.9993
30	297.3	2458.1	813.0	0.747	0.9992
40	517.3	2945.6	709.2	0.728	0.9992
50	970.9	3300.4	598.8	0.556	0.9991

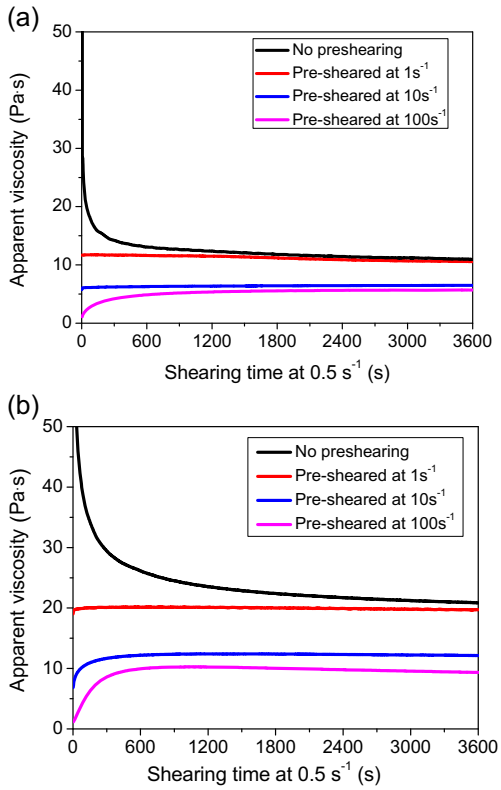

Fig. 12 Apparent viscosity recovery for crude oil and its emulsion gel at 0.5 s^{-1} after pre-sheared at different shear rates (31 °C): **a** water-free waxy crude oil gel and **b** emulsion gel with 40 % water cut

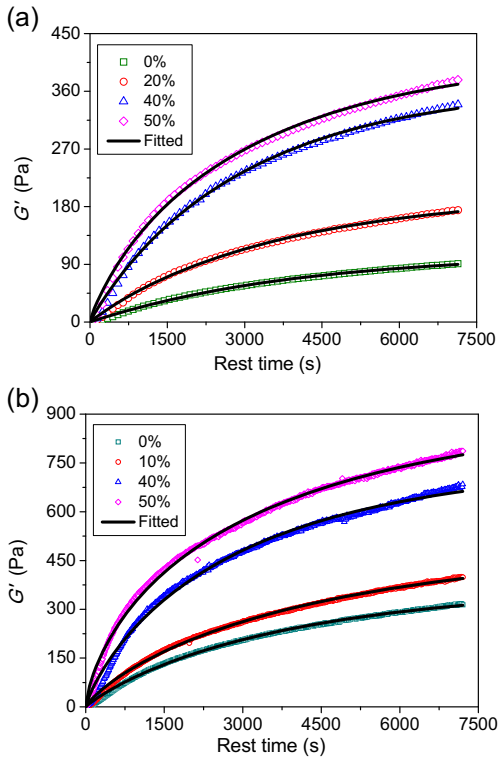

Fig. 13 Recovery of storage modulus with rest time at different temperatures for crude oil and its emulsion gels after sheared at 100 s^{-1} at **a** 31 and **b** 28 °C

Table 6 Fitted parameters of Eq. (1) for crude oil and its emulsion gels after sheared at different shear rates and temperatures

Temperature (°C)	Pre-shear rate (s^{-1})	Water cut (vol%)	G_0' (Pa)	G_∞' (Pa)	t_g (s)	d	R^2
31	100	0	0	108.6	4045.6	0.998	0.9987
		10	0	193.2	3941.5	0.973	0.9980
		20	0	203.9	3706.7	0.948	0.9982
		30	0	222.2	3213.2	0.921	0.9971
		40	0	371.9	2991.7	0.945	0.9976
		50	0	423.5	2956.1	0.835	0.9973
28	100	0	0	379.3	6038.3	0.807	0.9984
		10	0	508.9	4829.8	0.778	0.9983
		20	0	749.9	4433.2	0.755	0.9988
		30	0	757.7	3911.6	0.723	0.9953
		40	0	839.4	3892.6	0.697	0.9963
		50	0	942.0	3268.3	0.695	0.9969
31	10	0	0	119.4	5749.4	0.801	0.9992
		10	0	181.7	4553.5	0.776	0.9990
		20	0	212.2	4197.1	0.777	0.9994
		30	0	235.9	3858.3	0.810	0.9997
		40	0	373.5	3194.5	0.838	0.9985
		50	0	460.5	2980.0	0.788	0.9982

Table 7 manifests that the recovery rate constant k_{nb} decreases with increasing water cut, indicating that the yield stress recovers slower with higher water cut. This is contrary to the evolution of recovery rate of storage modulus with water cut in "Viscoelasticity." As shown above, the elasticity of the emulsion gels is quite low after structural breakdown, so the yield stress during the structural recovery period is mainly composed of viscous stress. Hence this result indicates that the recovery rate of the viscous part of the emulsion gels is reduced with increasing water cut.

By combining Fig. 15 and Table 7, it can be seen that the recovery proportion of the emulsion gels changes little with water cut when the rest time is 1 and 4 h, which illustrates again that the structural recovery degree is basically independent of water cut during this period. However, when the rest time is extended to 8 h, a tendency appears that the recovery proportion increases slightly with increasing water cut. Likewise, the calculated recovery proportion of the yield stress at infinite rest time ($\tau_{y\infty}$) by the Nguyen-Boger model

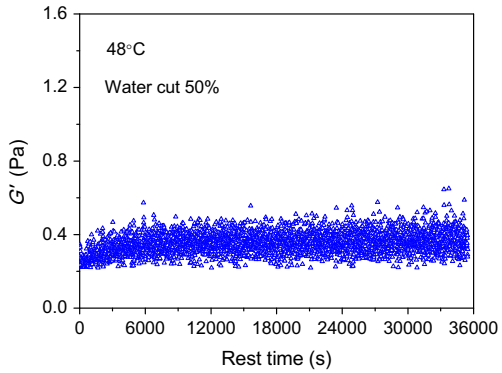

Fig. 14 Evolution of storage modulus with rest time above WAT after sheared at 100 s^{-1} for 30 min

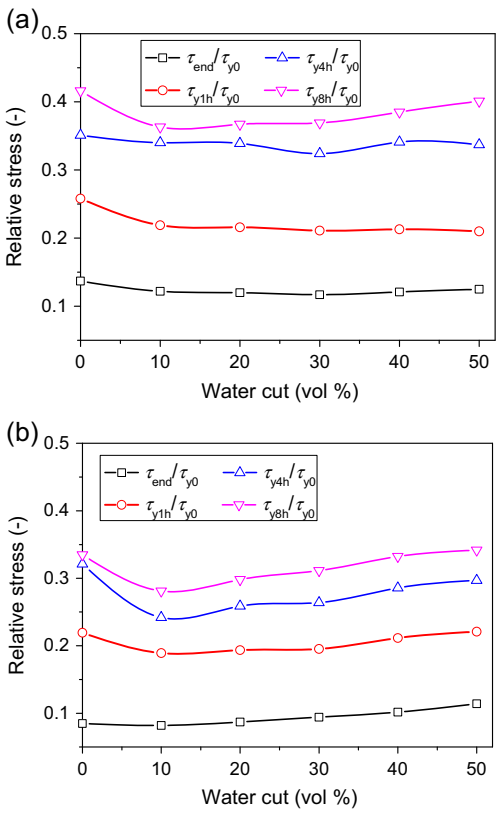

Fig. 15 Recovery proportion of yield stress vs. water cut after different rest time at 31 and 28 °C, respectively

Table 7 Fitted parameters of the Nguyen-Boger model for crude oil and its emulsion gels after different rest times and the recovery proportions of the yield stress

Temperature (°C)	Water cut (vol%)	$\tau_{y\infty}$ (Pa)	k_{nb} (1/h)	R^2	$\tau_{y\infty}/\tau_{y0}$
31	0	23.56	0.462	0.9998	0.413
	10	25.17	0.517	0.9988	0.369
	20	27.50	0.488	0.9995	0.373
	30	33.74	0.434	0.9869	0.387
	40	38.52	0.423	0.9992	0.396
	50	42.34	0.375	0.9999	0.398
28	0	66.90	0.7694	0.9997	0.334
	10	58.06	0.7679	0.9845	0.275
	20	63.64	0.6604	0.9506	0.289
	30	72.15	0.6042	0.9421	0.304
	40	78.60	0.5741	0.9504	0.324
	50	87.10	0.5641	0.9589	0.335

also increases slightly with increasing water cut. According to Haj-shafiei et al., the increase of the recovery proportion with water cut could be explained as follows: "the aging effect leads to enhanced synergy between growing Pickering crystals and dispersed droplets particularly at higher water cut" (Haj-shafiei et al. 2013).

When the temperature was lowered to 28 °C at which more wax was precipitated out, the recovery rate constant k_{nb} became higher than that at 31 °C, as shown in Table 7. This indicates that the recovery rate of yield stress is faster at lower temperature, which is contrary to the evolution of recovery rate of storage modulus with precipitated wax content in "Viscoelasticity" as well. Similar result was also reported by da Silva and Coutinho (2004). Compared with the yield stress recovery at 31 °C, the recovery proportion of both the crude oil and its emulsion gels are lower, indicating that the structure recoverability of crude oil and its emulsion gels weakens with increasing precipitated wax.

Furthermore, the yield strains of the first and the second yielding are shown in Fig. 16. As can be seen, the yield strain increases monotonically with increasing water cut, which has been discussed in our previous research (Sun et al. 2014). When the gel structure, whether it is the crude oil or the emulsion gel, yields again after resting for 1 h, its yield strain becomes higher than that of the first breakdown, and the higher the water cut is, the greater the increase of yield strain is. This may be attributed to the fact that the brittleness of the gel structure in the second yielding is reduced due to the decreased contribution of wax crystal structure. As the rest time goes on, the wax crystal network structure gradually recovers, leading to increased brittleness of the gel structure, so the yield strain is decreased accordingly. Interestingly, when the rest time is extended to 8 h, the yield strains of the crude oil and its emulsion gels below 30 % water cut are even lower than those of the first breakdown, which reflects the effect of wax aging again. To be specific, because the aging effect makes the wax crystal structure stiffer and more brittle, the joints between wax crystals will break down even when a relatively small strain is imposed (da Silva and Coutinho 2004; Haj-shafiei et al. 2013), manifesting the decrease of yield strain. By comparison, the contribution of wax crystal structure decreases in higher water cut emulsion gels, so the influence of the aging is not so obvious.

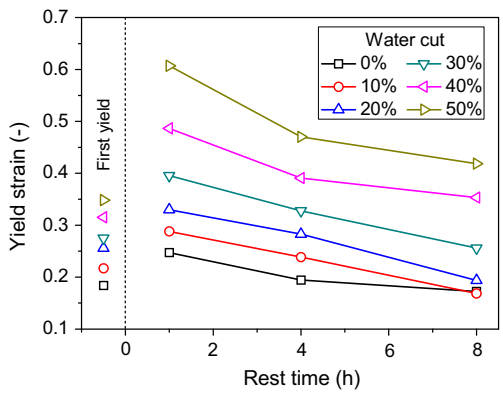

Fig. 16 Evolution of yield strain with rest time (31 °C)

Conclusions

After crude oil is emulsified and further gels, its structural behaviors will be changed. This study focused on the structural breakdown and recovery behaviors of waxy crude oil emulsion gels.

With the increasing contribution of dispersed droplets, the structural breakdown process gradually changes from sharp brittle fracture to ductile failure. Meanwhile, the thixotropy of emulsion gels becomes weaker with the increase of water cut because of the decreased contribution of the wax crystals to the structure.

The broken-down structure of waxy crude oil and its emulsion gels can only be recovered partially, and the structural

recovery behavior is related to the rate of pre-shear, water cut and temperature.

For both the crude oil and the emulsion gels, the gel structure recovers faster after pre-sheared at a higher shear rate. The apparent viscosity at 0.5 s^{-1} recovers obviously after highly pre-sheared at 100 s^{-1}, but barely recovers after pre-sheared at 1 s^{-1}. As to the recovery of storage modulus, the maximum storage moduli that can be recovered are roughly the same after the different pre-shear rates of 10 and 100 s^{-1}.

The existence of dispersed water droplets mainly affects the recovery rate of the emulsion gel. The recovery of structural storage modulus quickens while the recovery of yield stress slows with the increase of water cut. After the same pre-shearing, the absolute values of the recovered storage modulus and the yield stress still increase with increasing water cut, but the relative values, i.e., the recovery proportions, are nearly independent of the water cut within short rest time.

With the decrease of temperature, the recoverability of both storage modulus and yield stress for crude oil and its emulsion gels becomes weaker, and the recovery rate of storage modulus becomes slower while that of yield stress becomes faster, due to the increase of precipitated wax.

Acknowledgments Supports from the National Natural Science Foundation of China (grant no. 51134006) and the Science Foundation of China University of Petroleum-Beijing (grant no. LLYJ-2011-55) are gratefully acknowledged.

References

Cheng C, Boger DV, Nguyen QD (2000) Influence of thermal history on the waxy structure of statically cooled waxy crude oil. SPE J 5:148–157

da Silva JAL, Coutinho JAP (2004) Dynamic rheological analysis of the gelation behaviour of waxy crude oils. Rheol Acta 43:433–441

Davidson MR, Nguyen QD, Rønningsen HP (2007) Restart model for a multi-plug gelled waxy oil pipeline. J Petrol Sci Eng 59:1–16

de Kretser RG, Boger DV (2001) A structural model for the time-dependent recovery of mineral suspensions. Rheol Acta 40:582–590

de Oliveira MCK, Carvalho RM, Carvalho AB, Couto BC, Faria FR, Cardoso RL (2010) Waxy crude oil emulsion gel: impact on flow assurance. Energy Fuel 24:2287–2293

de Souza Mendes PR (2009) Modeling the thixotropic behavior of structured fluids. J Non-Newtonian Fluid Mech 164:66–75

de Souza Mendes PR (2011) Thixotropic elasto-viscoplastic model for structured fluids. Soft Matter 7:2471–2483

Dolz M, Hernández MJ, Delegido J, Alfaro MC, Muñoz J (2007) Influence of xanthan gum and locust bean gum upon flow and thixotropic behaviour of food emulsions containing modified starch. J Food Eng 81:179–186

Dullaert K, Mewis J (2006) A structural kinetics model for thixotropy. J Non-Newtonian Fluid Mech 139:21–30

Garcia PC, Whitby CP (2012) Laponite-stabilised oil-in-water emulsions: viscoelasticity and thixotropy. Soft Matter 8:1609–1615

Guo L, Zhang J, Han S, Teng H (2013) Evaluation of thixotropic models for waxy crudes based on stepwise shearing measurements. Petrol Sci Technol 31:895–901

Haj-shafiei S, Ghosh S, Rousseau D (2013) Kinetic stability and rheology of wax-stabilized water-in-oil emulsions at different water cuts. J Colloid Interface Sci 410:11–20

Hernández MJ, Dolz J, Delegido J, Cabeza C, Dolz M (2008) Thixotropic behavior of salad dressings stabilized with modified starch, pectin, and gellan gum. Influence of Temperature J Dispersion Sci Technol 29:213–219

Jia B, Zhang J (2012) Yield behavior of waxy crude gel: effect of isothermal structure development before prior applied stress. Ind Eng Chem Res 51:10977–10982

Kané M, Djabourov M, Volle JL, Lechaire JP, Frebourg G (2003) Morphology of paraffin crystals in waxy crude oils cooled in quiescent conditions and under flow. Fuel 82:127–135

Kané M, Djabourov M, Volle JL (2004) Rheology and structure of waxy crude oils in quiescent and under shearing conditions. Fuel 83: 1591–1605

Leong YK (1989) Rheology of unmodified and modified Victorian brown coal suspensions. Doctoral dissertation, University of Melbourne.

Levy G (1962) Rheology of thixotropic montmorillonite dispersions II. Kinetics of structural recovery. J Pharm Sci 51:952–957

Mewis J, Wagner NJ (2009) Thixotropy. Adv Colloid Interf Sci 147:214–227

Mujumdar A, Beris AN, Metzner AB (2002) Transient phenomena in thixotropic systems. J Non-Newtonian Fluid Mech 102:157–178

Nguyen QD, Boger DV (1985) Thixotropic behaviour of concentrated bauxite residue suspensions. Rheol Acta 24:427–437

Paso K, Silset A, Sørland G, Gonçalves MAL, Sjöblom J (2009) Characterization of the formation, flowability, and resolution of Brazilian crude oil emulsions. Energy Fuel 23:471–480

Rønningsen HP (1992) Rheological behaviour of gelled, waxy North Sea crude oils. J Petrol Sci Eng 7:177–213

Roussel N (2006) A thixotropy model for fresh fluid concretes: theory, validation and applications. Cem Concr Res 36:1797–1806

Saramito P (2009) A new elastoviscoplastic model based on the Herschel-Bulkley viscoplastic model. J Non-Newtonian Fluid Mech 158: 154–161

Sohm R, Tadros TF (1989) Viscoelastic properties of sodium montmorillonite (gelwhite H) suspensions. J Colloid Interface Sci 132:62–71

Solomon MJ, Almusallam AS, Seefeldt KF, Somwangthanaroj A, Varadan P (2001) Rheology of polypropylene/clay hybrid materials. Macromolecules 34:1864–1872

Sun G, Zhang J, Li H (2014) Structural behaviors of waxy crude oil emulsion gels. Energy Fuel 28:3718–3729

Tárrega A, Durán L, Costell E (2004) Flow behaviour of semi-solid dairy desserts. Effect of temperature. Int Dairy J 14:345–353

Teng H, Zhang J (2013a) A new thixotropic model for waxy crude. Rheol Acta 52:903–911

Teng H, Zhang J (2013b) Modeling the thixotropic behavior of waxy crude. Ind Eng Chem Res 52:8079–8089

Van Kessel T, Blom C (1998) Rheology of cohesive sediments: comparison between a natural and an artificial mud. J Hydraul Res 36:591–612

Vinay G, Wachs A, Agassant JF (2005) Numerical simulation of non-isothermal viscoplastic waxy crude oil flows. J Non-Newtonian Fluid Mech 128:144–1462

Vinay G, Wachs A, Frigaard I (2007) Start-up transients and efficient computation of isothermal waxy crude oil flows. J Non-Newtonian Fluid Mech 143:141–156

Visintin RFG, Lapasin R, Vignati E, D'Antona P, Lockhart TP (2005) Rheological behavior and structural interpretation of waxy crude oil gels. Langmuir 21:6240–6249

Visintin RFG, Lockhart TP, Lapasin R, D'Antona P (2008) Structure of waxy crude oil emulsion gels. J Non-Newtonian Fluid Mech 149: 34–39

Wardhaugh LT, Boger DV (1987) Measurement of the unique flow properties of waxy crude oils. Chem Eng Res Des 65:74–83

Wardhaugh LT, Boger DV (1991) The measurement and description of the yielding behavior of waxy crude oil. J Rheol 35:1121–1156

Webber RM (2001) Yield properties of wax crystal structures formed in lubricant mineral oils. Ind Eng Chem Res 40:195–203

Whitby CP, Garcia PC (2014) Time-dependent rheology of clay particle-stabilised emulsions. Appl Clay Sci 96:56–59

Yap J, Leong YK, Liu J (2011) Structural recovery behavior of barite-loaded bentonite drilling muds. J Petrol Sci Eng 78:552–558